

# Malachite Green Derivative–Functionalized Single Nanochannel: Light-and-pH Dual-Driven Ionic Gating

Liping Wen, Qian Liu, Jie Ma, Ye Tian, Cuihong Li, Zhishan Bo,\* and Lei Jiang\*

Biological nanochannels that can open and close in response to ambient stimuli play key roles in the proper performance of cellular and biological processes.<sup>[1]</sup> However, such kinds of nanochannels and their embedding lipid bilayers are susceptible to deterioration in changing external environments.<sup>[2]</sup> To overcome these difficulties, much effort has been focused on developing “abiotic” analogues, solid-state synthetic nanochannels that exhibit properties similar to those of the biological nanochannels but would be stable in a variety of conditions, such as temperature, pH, and mechanical stress.<sup>[2,3]</sup> So far, a variety of approaches and techniques have been used to prepare solid-state nanochannels: anodic oxidation,<sup>[4]</sup> focused-ion-beam etching,<sup>[5]</sup> electron beam technology,<sup>[6]</sup> track etching and so on.<sup>[7]</sup> The fabricated nanochannels, however, do not respond to external stimuli and they are not fully compatible with the application requirements. Functional groups that are introduced into synthetic nanochannels can respond to environmental stimuli, such as pH,<sup>[8]</sup> ions,<sup>[9]</sup> temperature,<sup>[10]</sup> ligands,<sup>[11]</sup> light,<sup>[12]</sup> and even electric fields,<sup>[13]</sup> and some of these responsive nanochannels have been used in sensing,<sup>[14]</sup> filtering,<sup>[15]</sup> and energy-conversion systems.<sup>[16]</sup>

In a nanochannel system with a fixed geometric structure and a given electrolyte, ionic transport properties are mainly controlled by the physical and chemical properties of the functionalizing stimuli-responsive materials inside the nanochannels, such as their configuration, charge, and wettability.<sup>[3b,17]</sup> In most cases, one stimulus-responsive molecule can respond to only one kind of external stimulus and realize a mono-responsive nanochannel. For example, a pH-gating ionic transport nanodevice has been developed by inserting the pH-sensitive polymer poly(acrylic acid) (PAA) into a synthetic nanochannel;<sup>[8b]</sup> thermally activated macromolecular gates have been produced by grafting temperature-responsive poly(*N*-isopropylacrylamide) (PNIPAM) into a synthetic nanochannel.<sup>[10]</sup> To obtain a dual-responsive nanochannel, two kinds of smart materials or one material with two functional

groups are needed to modify the same nanochannel. Recently, a series of pH-and-temperature dual-responsive ionic gates were developed by employing two kinds of responsive materials, such as PAA and PNIPAM,<sup>[17a]</sup> or one material with two functional groups, such as poly(NIPAM-*co*-AA)<sup>[18]</sup> or homopolymer poly[2-(dimethylamino) ethyl methacrylate] (PDMAEMA),<sup>[19]</sup> in a single nanochannel. However, the sensitivity and reversibility of these gates, which result mainly from configuration changes in a confined space, are not very efficient.<sup>[2]</sup>

In this Communication, we demonstrate an artificial functional nanochannel system as an ionic gate whose transport properties can be controlled by UV irradiation and pH, separately, while exhibiting ionic current rectifying behavior. This rectification is caused by an intrinsic asymmetry of the electrochemical potential of the channel.<sup>[20]</sup> For a cone-shaped nanochannel with permanent surface charges, the asymmetric shape allows the system to exhibit ionic current rectification because such a channel preferentially transports cations/anions from the small opening (tip) towards the large opening (base) side of the channel, even when the electrolyte is the same.<sup>[21]</sup> In this system, UV irradiation or reduction of the environmental pH can transform the surface from neutral (nonselective) to positively charged (anion-selective),<sup>[22]</sup> which changes the channel from the OFF state to the ON state. When UV irradiation was cut off or the environmental pH was increased, the channel became non-selective, and the OFF state was entered again. Even after several cycles there was no any decay in the ionic gating behavior; the functionalized nanochannel shows good reproducibility and reversibility and can be used as a switch in areas such as electronics, actuators, and biosensors.

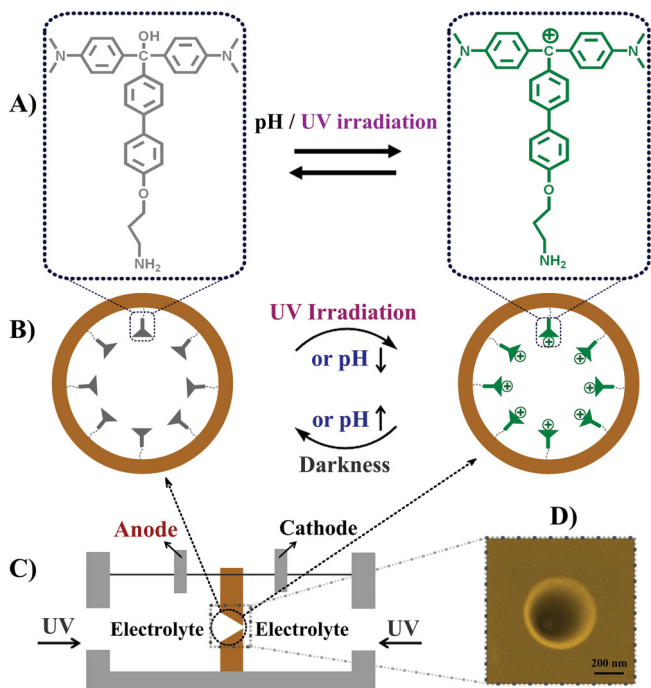
This function can be realized by grafting a novel, newly synthesized, pH-and-light dual-responsive molecule, malachite green derivative (MG-OH-NH<sub>2</sub>), onto the inner surface of a conical nanochannel. This channel was fabricated by a well-developed asymmetric ion track-etching technique on a polyimide film (PI, Hostaphan RN12 Hoechst, 12 μm thick, with a single ion track in the center); the diameters of the channel were conducted by a commonly used electrochemical method.<sup>[21a]</sup> The opening at the base was ≈550 nm, as was observed by scanning electron microscopy, and the diameter at the tip side was calculated to be ≈15 nm by an electrochemical measurement. The detailed procedure is described in the Experimental Section. MG-OH-NH<sub>2</sub> was added to the interior surface of the nanochannel by a two-step coupling reaction with 1-ethyl-3-(3-dimethylaminopropyl) carbodiimide (EDC) and *N*-hydroxysuccinimide (NHSS). As shown in **Scheme 1**, the MG-OH-NH<sub>2</sub> originally added to the nanochannel is neutral and hydrophobic, and the ions cannot be transported across the channel easily, resulting in an OFF state. When the

Dr. L. P. Wen, Dr. J. Ma, Dr. Y. Tian, Prof. L. Jiang  
Beijing National Laboratory for  
Molecular Sciences (BNLMS)  
Key Laboratory of Organic Solids  
Institute of Chemistry  
Chinese Academy of Sciences  
Beijing 100190, P. R. China  
E-mail: jianglei@iccas.ac.cn

Q. Liu, Dr. C. H. Li, Prof. Z. S. Bo  
College of Chemistry  
Beijing Normal University  
Beijing 100875, P. R. China  
E-mail: zsbo@bnu.edu.cn



DOI: 10.1002/adma.201202673



**Scheme 1.** Light- and pH- dual-driven ionic gate. A) The pH- and light-dependent equilibrium of malachite-green derivatives (MG-OH-NH<sub>2</sub>) that occurs on the inner surface of a polyimide single nanochannel. B) Simplified illustration indicating the charge changes occurring in the MG-OH-NH<sub>2</sub> layer upon variations in the environmental pH or light. C) The experimental setup of the electrochemical cell. D) Scanning electron microscopy (SEM) image, from the base side, of the conical nanochannel without MG-OH-NH<sub>2</sub> attached.

MG-OH-NH<sub>2</sub>-functionalized nanochannel system (MFNS) was put into an acid environment, or the MFNS was irradiated with UV light, the inner channel's surface became positively charged by releasing hydroxide ions, which resulted in an anion-selective, hydrophilic state. In this case, the anions prefer to flow from the tip to the base side of the channel, resulting in an ON state. If we put the MG cation-nanochannel system in an alkali environment or store the system in darkness, the generated MG cations will take up hydroxide ions and revert to the original neutral and hydrophobic MG-OH-NH<sub>2</sub>; in this case the OFF state will be recovered.

Ionic transport properties of the single nanochannel before and after MG-OH-NH<sub>2</sub> chemical modification have been examined by current measurements. **Figure 1A** shows current-voltage (*I*-*V*) properties of the nanochannel before chemical modification, measured in darkness or with UV irradiation filtered out. Reducing the pH changed the ionic current from rectifying to linear curves, owing to the anionic carboxyl (-COO<sup>-</sup>) groups at pH 7.0 and pH 10.2 and the neutral protonated state (-COOH) at pH 2.9; these results are similar to previous studies.<sup>[20a]</sup> After modification, the ionic transport behavior of the MFNS was observed as symmetric linear *I*-*V* curves (pH 7.0 and pH 10.2), owing to the neutral MG-OH-NH<sub>2</sub>, which diminished the negative charge inside the channel wall and led to an OFF state (Figure 1B). However, there was a remarkable difference: a tremendous increase in the ionic current rectification

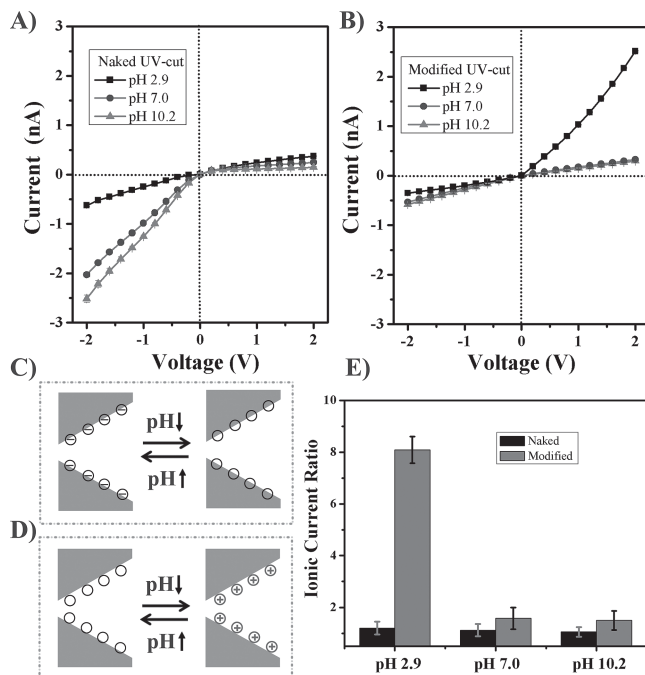


**Figure 1.** A,B) Current-voltage (*I*-*V*) curves of the single nanochannel before (A) and after (B) modification of the inner channel wall with MG-OH-NH<sub>2</sub>. *I*-*V* characteristics were recorded under symmetric electrolyte conditions (UV irradiation filtered out) at pH 2.9 (black squares), pH 7.0 (dark gray circles), and pH 10.2 (gray triangles). C,D) Explanation of the pH-tunable ionic gating before (C) and after (D) modification as being induced by the different polarities of the excess surface charge. E) Current rectification ratios  $R_D$  that were calculated as the current changes between -2 V and +2 V divided by the current measured at -2 V in the single conical nanochannel before (black) and after (gray) modification with MG-OH-NH<sub>2</sub> in different pH environments. The electrolyte solution was 0.1 M KCl with different pH values in both half-cells separated by the film. (Sample: base  $\approx$  550 nm, tip  $\approx$  15 nm, before chemical modification).

could be observed when the MFNS was placed in an acid environment (pH 2.9), giving the ON state. In this case, protons can combine with hydroxide ions coming from MG-OH-NH<sub>2</sub> and produce MG cations, thus the surface charge changes from neutral to positively charged. At the same time, the surface wettability transformed from hydrophobic to hydrophilic, and both surface charge and wettability contribute greatly to the ionic conductance.<sup>[2a,17f]</sup> This behavior can be explained by the mechanism shown in Figures 1C and D. The values can be quantified by the current rectifying ratio *R*, which was calculated as the current changes measured between two given voltages ( $\pm 2$  V) divided by the current measured at -2 V. The ratios that corresponded to a variation in the environmental pH only, in darkness (no UV), were defined as  $R_D$ , while the values measured in a neutral electrolyte, corresponding to a change in light irradiation only, were defined as  $R_N$ . As shown in Figure 1E,  $R_D$  of the naked nanochannel stayed around 1 for pH from 2.9 to 10.2. After modification,  $R_D$  of the MFNS at pH 10.2 was  $1.62 \pm 0.28$ , which is much lower than the  $8.05 \pm 0.68$  calculated at pH 2.9. This result verified that the asymmetric-response ionic transport property is caused by MG-OH-NH<sub>2</sub>, the charge of which changes in response to the ambient environmental pH.

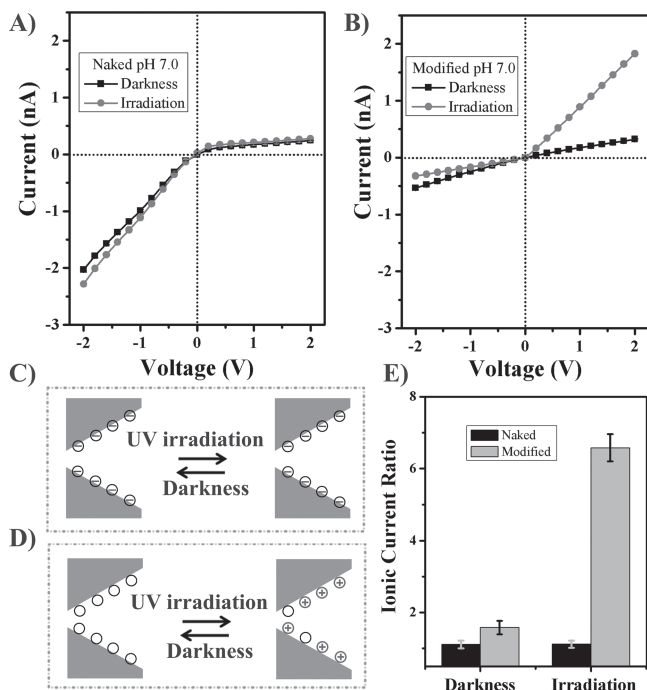


**Figure 2.** A,B)  $I$ - $V$  curves of the single nanochannel before (A) and after (B) modification with MG-OH-NH<sub>2</sub> on the inner channel wall.  $I$ - $V$  characteristics were recorded under symmetric electrolyte conditions (pH 7.0) in darkness (black squares) and under UV irradiation (gray circles). C,D) Explanation of the light-driven ionic gating before (C) and after (D) modification induced by the different polarities of the excess surface charge. E) Current rectification ratios that were calculated from the currents measured at  $\pm 2$  V in the single conical nanochannel before (black) and after (gray) modification with MG-OH-NH<sub>2</sub> under UV irradiation or without.

This pH-responsive property can also be characterized by contact angle measurements (Figure S3, Supporting Information) and X-ray photoelectron spectroscopy (XPS) analysis (Tables S1 and S2, Supporting Information).

In addition to being driven by the pH of the environment, the ionic current rectification property of this channel can also be activated by UV irradiation. As demonstrated in Figure 2A, before modification, UV irradiation had no influence on the rectification of the ionic current, which remained, even in a high conductivity neutral 0.1 M KCl solution. Having achieved closure of the MFNS, we set out to open the gate by UV irradiation (300–400 nm). When the UV lamp is off, the MFNS is in an OFF state in the neutral electrolyte regardless of the polarity of the voltage. After being irradiated with light from the UV lamp for  $\approx 5$  min, MG-OH-NH<sub>2</sub> will release hydroxide ions and produce MG cations, making the channel positively charged. Hence, the high conductance state is obtained as the anions are driven from the tip to the base by electrophoresis (Figure 2B). After 30 min in darkness, the MG cations have taken up the hydroxide ions completely and reverted to the original neutral and hydrophobic MG-OH-NH<sub>2</sub>; the low conductivity OFF state is obtained again. This behavior can be explained by the mechanism shown in Figures 2C and D. As shown in Figure 2E,  $R_N$  of the naked nanochannel stayed around 1 regardless of the irradiation of the channel. After modification,  $R_N$  of the MFNS

in UV irradiation was  $6.56 \pm 0.64$ , which is larger than  $1.55 \pm 0.47$  calculated for in the dark (Figure 2E). However, at pH 2.9 the channel is always positively charged regardless of UV irradiation, because hydroxide ions in MG-OH-NH<sub>2</sub> can be easily released in an acid environment. At pH 10.2, the channel is always in the neutral state regardless of UV irradiation of the MFNS, because more hydroxide ions in the alkali environment can react with MG cations and revert to the original neutral MG-OH-NH<sub>2</sub> (Figure S4 in the Supporting Information). Compared with the ratios calculated from the pH-stimulus system, there is a small decrease for the UV-stimulus system, which may be ascribed to the difference in driving mechanism, in that control is not as efficient for a remote noncontact technique as for a contact-mode technique in a confined space.

To determine the stability and the responsive switching ability of the MFNS, further studies have been done, which are shown in Figure 3. Before modification (naked; gray circles), there was

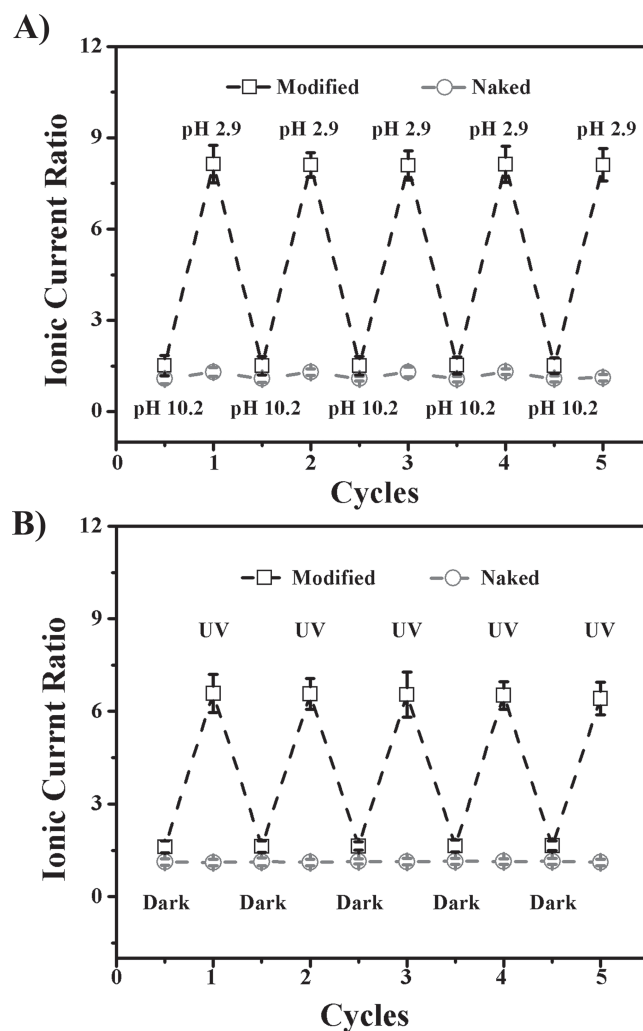


**Figure 3.** Stability and responsive switching ability of the dual-driven nanochannel system for variation of the pH (A) and light (B): reversible variation of the ionic current rectification ratios of the single nanochannel before (gray circles) and after (squares) modification under stimulation with pH and UV irradiation.

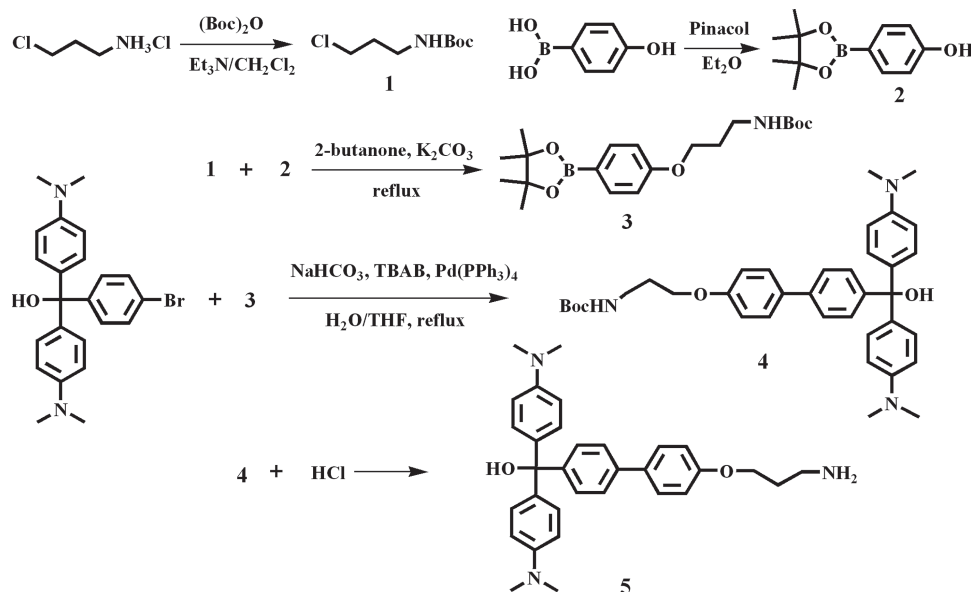


**Figure 4.** The synthetic route to MG-OH-NH<sub>2</sub>, molecule 5 (Pinacol: 2,3-dimethyl-2,3-butanediol).

almost no change in the current ratio regardless of variation of pH and UV irradiation; it is stable. Thus, such a material can be used as an ideal platform for developing smart nanochannel systems. The responsive switching ability of the MFNS (black squares) upon cyclic variation of either the pH or UV irradiation reflects good reproducibility and reversibility of the asymmetric responsive nanochannels. The time scale of each cycle of the responsive switching experiment was about 35 min, a result of the behavior of MG-OH-NH<sub>2</sub>, which is much faster than the previously reported biomimetic systems, because surface charges generated by smart materials are much easier to realize in a confined region than a change in configuration when activated by external stimuli. Therefore, the sensitivity and reversibility of the MFNS are highly efficient compared with those of systems based on conformation changes in confined regions.

In summary, we have demonstrated the construction of a highly efficient and perfectly reversible pH-and-light dual-driven ionic gate based on a single conical nanochannel fabricated in a PI membrane. MG-OH-NH<sub>2</sub> as the active element was first synthesized and then incorporated into the channel by directly exploiting the carboxyl groups generated during the track-etching process. The switching between the OFF state and the ON state is mainly dependent on the surface charge transition brought about by MG-OH-NH<sub>2</sub> activated by the variation of pH and UV irradiation, which makes it easy to realize in confined spaces. Moreover, compared with fragile biological nanochannels in living systems, this “abiotic” equivalent is robust and has the advantage that it does not have to work in the lipid environment. Therefore, such a pH-and-light dual-driven ionic gate can be used as a switch and may find applications in areas such as electronics, actuators, and biosensors.

## Experimental Section

**Materials:** The malachite green derivative MG-OH-NH<sub>2</sub> shown in **Figure 4** was synthesized and used for the functionalization of track-etched nanochannel. This compound was purified and characterized by <sup>1</sup>H NMR, <sup>13</sup>C NMR, and matrix-assisted laser desorption/ionization time-of-flight mass spectrometry (MALDI-TOF-MS). The synthesis of malachite green derivative 5 was performed as given below. The absorption spectra of MG-OH-NH<sub>2</sub> and its corresponding product are shown in Figure S1 (Supporting Information). Other chemicals were analytical-grade reagents and were used as received. All aqueous solutions were prepared with deionized water.

**Synthesis of tert-Butyl 3-chloropropylcarbamate (1):** Et<sub>3</sub>N (12.9 mL, 0.092 mol) was added slowly into a solution of 3-chloropropan-1-amine hydrochloride (10 g, 0.076 mol) in dichloromethane (DCM; 50 mL). The resulting solution was cooled to 0 °C with an ice bath, then a solution of di-tert-butyl dicarbonate ((Boc)<sub>2</sub>O; 16.8 g, 0.077 mol) in DCM (50 mL) was added dropwise and the reaction was stirred at 0 °C overnight. After the reaction, the mixture was washed with a solution of HCl (pH 1) three times and dried with anhydrous MgSO<sub>4</sub>. Removal of the solvent by rotary evaporator afforded compound 1 as a yellow oil (14 g, 98%). <sup>1</sup>H NMR (CD<sub>3</sub>Cl, 400 MHz): δ 5.15 (s, 1H), 3.61–3.57 (t, 2H), 3.29–3.25 (m, 2H), 2.00–1.94 (m, 2H), 1.44 (s, 9H); <sup>13</sup>C NMR (100 MHz, CDCl<sub>3</sub>): δ 156.07, 79.22, 42.32, 37.83, 32.61, 28.32.

**Synthesis of tert-Butyl 3-(4-(4,4,5,5-tetramethyl-1,3,2-dioxaborolan-2-yl)phenoxy)propylcarbamate (3):** A mixture of 1 (3.16 g, 0.016 mol), 2 (3.00 g, 0.014 mol), 2-butanone (150 mL), 18-crown-6 (3.95 g, 0.015 mol), KI (2.49 g, 0.015 mol), and K<sub>2</sub>CO<sub>3</sub> (5.64 g, 0.041 mol) was heated at reflux and stirred under nitrogen for 24 h. The solvent was removed under reduced pressure, the residue was partitioned between water and CH<sub>2</sub>Cl<sub>2</sub>, the organic layer was separated, the aqueous layer was extracted with CH<sub>2</sub>Cl<sub>2</sub>, and the combined organic layers were dried over anhydrous Na<sub>2</sub>SO<sub>4</sub> and evaporated to dryness. The residue was chromatographically purified on silica gel, eluting with petroleum ether/ethyl acetate (4:1, v:v), to afford 3 as a white solid (3.47 g, 67.5%). <sup>1</sup>H NMR (CD<sub>3</sub>Cl, 400 MHz): δ 7.75–7.73 (d, 2H), 6.89–6.87 (d, 2H), 4.06–4.03 (t, 2H), 3.34–3.32 (m,

2H), 2.00–1.96 (m, 2H), 1.44 (s, 9H), 1.33 (s, 12H);  $^{13}\text{C}$  NMR (100 MHz,  $\text{CDCl}_3$ ):  $\delta$  161.40, 156.11, 136.60, 136.56, 113.81, 83.61, 79.23, 65.58, 37.95, 29.52, 28.45, 24.90.

**Synthesis of Malachite Green Derivative 4:** A mixture of **3** (500 mg, 1.33 mmol), (4-bromophenyl)bis(4-(dimethylamino)phenyl)methanol (511 mg, 1.20 mmol), tetrahydrofuran (THF; 50 mL),  $\text{H}_2\text{O}$  (10 mL), tetrabutylammonium bromide (TBAB; 386 mg, 1.19 mmol), and  $\text{NaHCO}_3$  (1.01 g, 12.02 mmol) was degassed before and after  $\text{Pd}(\text{PPh}_3)_4$  (40 mg, 0.03 mmol) was added. The mixture was then heated at reflux and stirred under nitrogen for 2 days. After cooling to room temperature, the mixture was partitioned between water and diethyl ether, the organic layer was separated, the aqueous layer was extracted with diethyl ether (100 mL  $\times$  3), and the combined organic layers were dried over anhydrous  $\text{MgSO}_4$  and evaporated to dryness. The residue was purified chromatographically on silica gel to afford **4** as a green oil (331 mg, 40%).  $^1\text{H}$  NMR ( $\text{CD}_3\text{Cl}$ , 400 MHz):  $\delta$  7.52–7.45 (m, 4H), 7.36–7.34 (d, 2H), 7.16–7.13 (d, 4H), 6.95–6.93 (d, 2H), 6.68–6.66 (d, 4H), 4.07–4.04 (t, 2H), 3.35–3.32 (m, 2H), 2.94 (s, 12H), 2.00–1.96 (m, 2H), 1.45 (s, 9H).  $^{13}\text{C}$  NMR (100 MHz,  $\text{CDCl}_3$ ):  $\delta$  158.22, 156.07, 149.50, 146.49, 138.91, 135.60, 128.81, 128.03, 125.87, 114.73, 111.76, 81.41, 79.21, 67.93, 40.55, 38.07, 29.55, 28.41.

**Synthesis of Malachite Green Derivative 5:** A mixture of **4** (300 mg, 0.50 mmol), THF (30 mL), and HCl (8 mL, 36%) was stirred at room temperature for 12 h, and the resulted precipitate was collected by filtration. The crude product was chromatographically purified on silica gel, eluting with  $\text{CH}_2\text{Cl}_2$ , increasing to  $\text{CH}_2\text{Cl}_2/\text{CH}_3\text{OH}$  (1:1, v/v) to afford the crude product. The crude product was dissolved in  $\text{CH}_2\text{Cl}_2$  (100 mL) and filtered through filter paper; the collected filtrate was evaporated to dryness to afford the desired malachite green derivative **5** as a green oil.  $^1\text{H}$  NMR ( $\text{CD}_3\text{Cl}$ , 400 MHz):  $\delta$  7.51–7.45 (m, 4H), 7.35–7.33 (d, 2H), 7.16–7.14 (d, 4H), 6.96–6.94 (d, 2H), 6.69–6.67 (d, 4H), 4.08–4.06 (m, 2H), 3.35–3.32 (m, 2H), 2.94 (s, 12H), 2.00–1.96 (m, 2H);  $^{13}\text{C}$  NMR (100 MHz,  $\text{CDCl}_3$ ):  $\delta$  153.35, 149.03, 135.66, 132.78, 130.28, 128.91, 128.30, 126.20, 114.84, 111.77, 81.45, 58.93, 45.90, 42.27, 40.80. MS (MALDI-TOF)  $m/z$  478.4 [(M–OH) $^+$ , the cation of lost hydroxide].

**Nanochannel Fabrication and Characterization:** The single conical nanochannel was prepared with a polyimide (PI, 12  $\mu\text{m}$  thick) membrane, which was irradiated with single swift heavy ions (Au) of energy 11.4 MeV per nucleon at the UNILAC linear accelerator (GSI, Darmstadt, Germany). Then the ion track polymer membrane was chemically etched at a fixed temperature (about 333 K) from one side with 13% NaClO, whereas the other side of the cell contained 1 M KI to neutralize the etchant as soon as the pore opened. After etching had finished, the film was soaked in MilliQ water (18.2 M $\Omega$ ) to remove residual salts. The diameter  $D$  of the large opening (base) of the conical nanochannel was determined by scanning electron microscopy (SEM) in parallel etching experiments; the diameter  $d_{\text{tip}}$  of the small opening (tip) was evaluated from an electrochemical measurement of the ionic conductance of the nanochannel filled with 1 M potassium chloride solution as electrolyte by means of (Figure S2, Supporting Information)

$$d_{\text{tip}} = \frac{4LI}{\pi k(c)UD} \quad (1)$$

where  $d_{\text{tip}}$  is the tip diameter;  $D$  is the base diameter ( $\approx 550$  nm);  $k(c)$  is the specific conductivity of the electrolyte (for 1 M KCl solution at 25  $^\circ\text{C}$   $k(c) = 0.11173 \Omega^{-1}\text{cm}^{-1}$ );  $L$  is the length of the channel, which can be approximated to the thickness of the membrane after chemical etching ( $\approx 12$   $\mu\text{m}$ ); and  $U$  and  $I$  are the applied voltage and measured ionic current in the pore conductivity measurement, respectively. In this work, the applied voltage and measured ionic current were 0.2 V and 1.2 nA, respectively. From Equation (1) and the corresponding parameters we can estimate the tip diameter of the ion track-etched nanochannel; it is around 15 nm. The etching and characterizing conductivity cell with an  $I$ - $V$  characterization of the naked nanochannel in the PI membrane are shown in Figure S2 (Supporting Information).

**Nanochannel Functionalization:** The chemical functionalization of carboxyl (–COOH) groups generated on the channel surface during the

ionic track-etching process was effected by the following procedure. The first step was the activation of these groups into amine-reactive esters by means of carbodiimide coupling chemistry. Then, these reactive esters were further condensed with malachite green derivatives through the formation of covalent bonds. For the activation of carboxyl groups into NHSS-ester, the PI film containing a single channel was exposed to an aqueous solution of 15 mg EDC and 3 mg NHSS for 1 h at room temperature. After they had been washed with distilled water, the samples were further treated with 5 mM malachite green derivatives overnight. Finally, functionalized channels were washed several times with distilled water.

**Current–Voltage Recordings:** The properties of the system were studied by measuring the ionic current through unmodified (naked) and modified channels. The ionic current was measured by a Keithley 6487 picoammeter (Keithley Instruments, Cleveland, OH). A single channel in the center of the PI membrane was mounted between the two chambers of the etching cell, which can be irradiated from the sidewall. Ag/AgCl electrodes were used to apply a transmembrane potential across the film (anode facing the base of the nanochannel), and both halves of the cell were filled with 0.1 M KCl. The main transmembrane potential used in this work was a scanning voltage that varied from –2 V to +2 V with a period of 40 s. The process and conditions of all the measurements mentioned in this Communication were the same, unless stated otherwise, and each test was repeated 8 times to obtain the average current value at different voltages.

## Supporting Information

Supporting Information is available from the Wiley Online Library or from the author.

## Acknowledgements

The authors thank the Material Science Group of GSI (Darmstadt, Germany) for providing the ion-irradiated samples. This work was supported by the National Research Fund for Fundamental Key Projects (2011CB935703, 2011CB935704, 2010CB934700), National Natural Science Foundation (21171171, 91127025, 20920102036, 21121001), and the Key Research Program of the Chinese Academy of Sciences (KJZD-EW-M01).

Received: July 2, 2012

Revised: September 18, 2012

Published online:

- [1] a) X. Hou, H. Zhang, L. Jiang, *Angew. Chem. Int. Ed.* **2012**, *51*, 5296; b) X. Hou, L. Jiang, *ACS Nano* **2009**, *3*, 3339; c) B. Hille, *Ion Channels of Excitable Membranes*, 3rd Ed., Sinauer Associates, Sunderland, MA **2001**; d) E. Perozo, D. M. Cortes, P. Somporpnisut, A. Kloda, B. Martinac, *Nature* **2002**, *418*, 942; e) E. Gouaux, R. MacKinnon, *Science* **2005**, *310*, 1461.
- [2] a) X. Hou, W. Guo, L. Jiang, *Chem. Soc. Rev.* **2011**, *40*, 2385; b) L. Wen, Y. Tian, J. Ma, J. Zhai, L. Jiang, *Phys. Chem. Chem. Phys.* **2012**, *14*, 4027.
- [3] a) S. Howorka, Z. Siwy, *Chem. Soc. Rev.* **2009**, *38*, 2360; b) M. Ali, B. Yameen, J. Cervera, P. Ramirez, R. Neumann, W. Ensinger, W. Knoll, O. Azzaroni, *J. Am. Chem. Soc.* **2010**, *132*, 8338.
- [4] W. Lee, K. Schwirn, M. Steinhart, E. Pippel, R. Scholz, U. Gösele, *Nat. Nanotechnol.* **2008**, *3*, 234.
- [5] J. Li, D. Stein, C. McMullan, D. Branton, M. J. Aziz, J. A. Golovchenko, *Nature* **2001**, *412*, 166.
- [6] A. J. Storm, J. H. Chen, X. S. Ling, H. W. Zandbergen, C. Dekker, *Nat. Mater.* **2003**, *2*, 537.

- [7] a) J. Wu, A. Eisenberg, *J. Am. Chem. Soc.* **2006**, *128*, 2880; b) Y. Lu, R. Ganguli, C. A. Drewien, M. T. Anderson, C. J. Brinker, W. Gong, Y. Guo, H. Soye, B. Dunn, M. H. Huang, J. I. Zink, *Nature* **1997**, *389*, 364; c) Z. S. Siwy, M. Davenport, *Nat. Nanotechnol.* **2010**, *5*, 697.
- [8] a) F. Xia, W. Guo, Y. Mao, X. Hou, J. Xue, H. Xia, L. Wang, Y. Song, H. Ji, Q. Ouyang, Y. Wang, L. Jiang, *J. Am. Chem. Soc.* **2008**, *130*, 8345; b) X. Hou, Y. Liu, H. Dong, F. Yang, L. Li, L. Jiang, *Adv. Mater.* **2010**, *22*, 2440; c) Z. S. Siwy, P. Apel, D. Baur, D. D. Dobrev, Y. E. Korchev, R. Neumann, R. Spohr, C. Trautmann, K.-O. Voss, *Surf. Sci.* **2003**, *532–535*, 1061; d) I. Vlasiouk, Z. S. Siwy, *Nano Lett.* **2007**, *7*, 552; e) B. Yameen, M. Ali, R. Neumann, W. Ensinger, W. Knoll, O. Azzaroni, *Nano Lett.* **2009**, *9*, 2788; f) B. Yameen, M. Ali, R. Neumann, W. Ensinger, W. Knoll, O. Azzaroni, *J. Am. Chem. Soc.* **2009**, *131*, 2070; g) M. Wanunu, A. Meller, *Nano Lett.* **2007**, *7*, 1580; h) R. Fan, S. Huh, R. Yan, J. Arnold, P. Yang, *Nat. Mater.* **2008**, *7*, 303; i) G. Wang, B. Zhang, J. R. Wayment, J. M. Harris, H. S. White, *J. Am. Chem. Soc.* **2006**, *128*, 7679; j) M. Ali, P. Ramirez, S. Mafé, R. Neumann, W. Ensinger, *ACS Nano* **2009**, *3*, 603; k) G. Wang, A. K. Bohaty, I. Zharov, H. S. White, *J. Am. Chem. Soc.* **2006**, *128*, 13553.
- [9] a) X. Hou, W. Guo, F. Xia, F.-Q. Nie, H. Dong, Y. Tian, L. Wen, L. Wang, L. Cao, Y. Yang, J. Xue, Y. Song, Y. Wang, D. Liu, L. Jiang, *J. Am. Chem. Soc.* **2009**, *131*, 7800; b) Y. Tian, X. Hou, L. Wen, W. Guo, Y. Song, H. Sun, Y. Wang, L. Jiang, D. Zhu, *Chem. Commun.* **2010**, *46*, 1682; c) M. R. Powell, M. Sullivan, I. Vlasiouk, D. Constantin, O. Sudre, C. C. Martens, R. S. Eisenberg, Z. S. Siwy, *Nat. Nanotechnol.* **2008**, *3*, 51; d) Y. He, D. Gillespie, D. Boda, I. Vlasiouk, R. S. Eisenberg, Z. S. Siwy, *J. Am. Chem. Soc.* **2009**, *131*, 5194; e) O. Braha, L.-Q. Gu, L. Zhou, X. Lu, S. Cheley, H. Bayley, *Nat. Biotechnol.* **2000**, *18*, 1005.
- [10] a) B. Yameen, M. Ali, R. Neumann, W. Ensinger, W. Knoll, O. Azzaroni, *Small* **2009**, *5*, 1287; b) W. Guo, H. Xia, F. Xia, X. Hou, L. Cao, L. Wang, J. Xue, G. Zhang, Y. Song, D. Zhu, Y. Wang, L. Jiang, *ChemPhysChem* **2010**, *11*, 859.
- [11] a) C. Han, X. Hou, H. Zhang, W. Guo, H. Li, L. Jiang, *J. Am. Chem. Soc.* **2011**, *133*, 7644; b) E. A. Heins, L. A. Baker, Z. S. Siwy, M. O. Mota, C. R. Martin, *J. Phys. Chem. B* **2005**, *109*, 18400; c) A. E. Abelow, O. Schepelina, R. J. White, A. Vallee-Belisle, K. W. Plaxco, I. Zharov, *Chem. Commun.* **2010**, *46*, 7984.
- [12] a) L. Wen, J. Ma, Y. Tian, J. Zhai, L. Jiang, *Small* **2012**, *8*, 838; b) N. Liu, D. R. Dunphy, P. Atanassov, S. D. Bunge, Z. Chen, G. P. López, T. J. Boyle, C. J. Brinker, *Nano Lett.* **2004**, *4*, 551; c) A. Koçer, M. Walko, W. Meijberg, B. L. Feringa, *Science* **2005**, *309*, 755; d) I. Vlasiouk, C.-D. Park, S. A. Vail, D. Gust, S. Smirnov, *Nano Lett.* **2006**, *6*, 1013; e) G. Nagel, T. Szellas, W. Huhn, S. Kateriya, N. Adeishvili, P. Berthold, D. Ollig, P. Hegemann, E. Bamberg, *Proc. Natl. Acad. Sci. USA* **2003**, *100*, 13940; f) M. Zhang, X. Hou, J. Wang, Y. Tian, X. Fan, J. Zhai, L. Jiang, *Adv. Mater.* **2012**, *24*, 2424.
- [13] a) E. Kalman, O. Sudre, I. Vlasiouk, Z. S. Siwy, *Anal. Bioanal. Chem.* **2009**, *394*, 413; b) C. C. Harrell, P. Kohli, Z. Siwy, C. R. Martin, *J. Am. Chem. Soc.* **2004**, *126*, 15646.
- [14] a) E. A. Heins, Z. S. Siwy, L. A. Baker, C. R. Martin, *Nano Lett.* **2005**, *5*, 1824; b) R. E. Gyurcsányi, *Trends Anal. Chem.* **2008**, *27*, 627; c) Z. S. Siwy, M. Davenport, *Nat. Nanotechnol.* **2010**, *5*, 174; d) S. Wen, T. Zeng, L. Liu, K. Zhao, Y. Zhao, X. Liu, H.-C. Wu, *J. Am. Chem. Soc.* **2011**, *133*, 18312; e) Z. Chen, Y. Jiang, D. R. Dunphy, D. P. Adams, C. Hodges, N. Liu, N. Zhang, G. Xomeritakis, X. Jin, N. R. Aluru, S. J. Gaik, H. W. Hillhouse, C. J. Brinker, *Nat. Mater.* **2010**, *9*, 667; f) D. K. Lathrop, E. N. Ervin, G. A. Barrall, M. G. Keehan, R. Kawano, M. A. Krupka, H. S. White, A. H. Hibbs, *J. Am. Chem. Soc.* **2010**, *132*, 1878; g) C. Dekker, *Nat. Nanotechnol.* **2007**, *2*, 209; h) B. Zhang, Y. Zhang, H. S. White, *Anal. Chem.* **2004**, *76*, 6229; i) A. Mara, Z. Siwy, C. Trautmann, J. Wan, F. Kamme, *Nano Lett.* **2004**, *4*, 497; j) J. Li, M. Gershow, D. Stein, E. Brandin, J. A. Golovchenko, *Nat. Mater.* **2003**, *2*, 611; k) A. J. Storm, C. Storm, J. Chen, H. Zandbergen, J.-F. Joanny, C. Dekker, *Nano Lett.* **2005**, *5*, 1193; l) C. R. Martin, Z. S. Siwy, *Science* **2007**, *317*, 331; m) L.-Q. Gu, O. Braha, S. Conlan, S. Cheley, H. Bayley, *Nature* **1999**, *398*, 686; n) E. C. Yusko, J. M. Johnson, S. Majid, P. Prangkio, R. C. Rollings, J. Li, J. Yang, M. Mayer, *Nat. Nanotechnol.* **2011**, *6*, 253.
- [15] a) B. Corry, *J. Phys. Chem. B* **2007**, *112*, 1427; b) L. A. Baker, S. P. Bird, *Nat. Nanotechnol.* **2008**, *3*, 73; c) E. N. Savariar, K. Krishnamoorthy, S. Thayumanavan, *Nat. Nanotechnol.* **2008**, *3*, 112; d) H. Gu, S. Faucher, S. Zhu, *AIChE J.* **2010**, *56*, 1684.
- [16] a) L. Wen, X. Hou, Y. Tian, J. Zhai, L. Jiang, *Adv. Funct. Mater.* **2010**, *20*, 2636; b) W. Guo, L. Cao, J. Xia, F.-Q. Nie, W. Ma, J. Xue, Y. Song, D. Zhu, Y. Wang, L. Jiang, *Adv. Funct. Mater.* **2010**, *20*, 1339; c) F. H. J. van der Heyden, D. Stein, C. Dekker, *Phys. Rev. Lett.* **2005**, *95*, 116104; d) F. H. J. van der Heyden, D. J. Bonthuis, D. Stein, C. Meyer, C. Dekker, *Nano Lett.* **2006**, *6*, 2232; e) F. H. J. van der Heyden, D. J. Bonthuis, D. Stein, C. Meyer, C. Dekker, *Nano Lett.* **2007**, *7*, 1022; f) P. Banerjee, I. Perez, L. Henn-Lecordier, S. B. Lee, G. W. Rubloff, *Nat. Nanotechnol.* **2009**, *4*, 292; g) L. Cao, W. Guo, W. Ma, L. Wang, F. Xia, S. Wang, Y. Wang, L. Jiang, D. Zhu, *Energy Environ. Sci.* **2011**, *4*, 2259.
- [17] a) X. Hou, F. Yang, L. Li, Y. Song, L. Jiang, D. Zhu, *J. Am. Chem. Soc.* **2010**, *132*, 11736; b) P. Ramirez, V. Gómez, J. Cervera, B. Schiedt, S. Mafé, *J. Chem. Phys.* **2007**, *126*, 194703; c) K. Zhou, M. L. Kovarik, S. C. Jacobson, *J. Am. Chem. Soc.* **2008**, *130*, 8614; d) D. Stein, M. Kruithof, C. Dekker, *Phys. Rev. Lett.* **2004**, *93*, 035901; e) C. C. Striemer, T. R. Gaborski, J. L. McGrath, P. M. Fauchet, *Nature* **2007**, *445*, 749; f) S. N. Smirnov, I. V. Vlasiouk, N. V. Lavrik, *ACS Nano* **2011**, *5*, 7453; g) R. Karnik, K. Castelino, R. Fan, P. Yang, A. Majumdar, *Nano Lett.* **2005**, *5*, 1638.
- [18] W. Guo, H. Xia, L. Cao, F. Xia, S. Wang, G. Zhang, Y. Song, Y. Wang, L. Jiang, D. Zhu, *Adv. Funct. Mater.* **2010**, *20*, 3561.
- [19] L.-X. Zhang, S.-L. Cai, Y.-B. Zheng, X.-H. Cao, Y.-Q. Li, *Adv. Funct. Mater.* **2011**, *21*, 2103.
- [20] a) Z. Siwy, A. Fuliński, *Phys. Rev. Lett.* **2002**, *89*, 198103; b) R. D. Astumian, *Science* **1997**, *276*, 917.
- [21] a) P. Y. Apel, Y. E. Korchev, Z. S. Siwy, R. Spohr, M. Yoshida, *Nucl. Instrum. Methods Phys. Res., Sect. B* **2001**, *184*, 337; b) Z. Siwy, Y. Gu, H. A. Spohr, D. Baur, A. Wolf-Reber, R. Spohr, P. Apel, Y. E. Korchev, *Europhys. Lett.* **2002**, *60*, 349; c) Z. S. Siwy, *Adv. Funct. Mater.* **2006**, *16*, 735; d) J. Cervera, A. Alcaraz, B. Schiedt, R. Neumann, P. Ramirez, *J. Phys. Chem. C* **2007**, *111*, 12265; e) Z. Siwy, I. D. Kosińska, A. Fuliński, C. R. Martin, *Phys. Rev. Lett.* **2005**, *94*, 048102.
- [22] a) Y. Jiang, P. Wan, M. Smet, Z. Wang, X. Zhang, *Adv. Mater.* **2008**, *20*, 1972; b) M. Irie, *J. Am. Chem. Soc.* **2002**, *105*, 2078.